# An Improved Technique for Permittivity Measurements Using a Coaxial Probe

David V. Blackham, *Member, IEEE*, and Roger D. Pollard, *Fellow, IEEE*

***Abstract*—An enhanced model for an open-ended coaxial probe used for making permittivity measurements is presented. A permittivity measurement system consisting of the coaxial probe and a network analyzer is described including details of the error correction and curve fitting techniques. Determination of the percent dissolved solids in fructose solutions from permittivity measurements is presented as example of the usefulness of the coaxial probe/network analyzer measurement system.**

***Index Terms*— Coaxial probe, moisture content, permittivity measurement, refresh calibration, vector network analyzer.**

## I. Introduction

THE COAXIAL probe combined with a vector network analyzer is useful in measuring the permittivity of nonmagnetic materials. Fundamental to the use of the coaxial probe is an accurate model relating the reflection coefficient at the coaxial probe aperture to the permittivity of the material contacting the probe. Several approaches to modeling the probe have been taken ranging from equivalent circuit models to variational techniques. The simplicity of the lumped circuit models [1]–[5] provide for the fastest computation over a limited range of frequency and permittivity for which the lumped circuit model is valid. Variational techniques provide the best accuracy at the expense of computational speed [6], [7]. Others have provided detailed comparisons of various probe models [8]–[10]. The model used in this paper is an optimized blend of speed, range and accuracy with broad applicability. An alternate model based on fitting a full-wave moment method to a rational function also addresses the issue of range and accuracy at a reasonable speed [11], [12]

Examples of the usefulness of this technique are provided by measurements of liquids and by assessing the percent dissolved solids from permittivity measurement of solutions. The coaxial probe allows a wide frequency spectrum to be used rather than a more traditional approach of using measurements at a single frequency [13]. In some cases resonant cavities are used because they have better sensitivity than broadband techniques although restricted to a single frequency. In this paper measured data over a range of frequencies are curve fitted to an expression resulting in improved resolution of the percent dissolved solids.

Manuscript received January 3, 1995.

D. V. Blackham is with the Microwave Instruments Division, Hewlett Packard Co., Santa Rosa, CA 95403 USA (e-mail: daveb@sr.hp.com).

R. D. Pollard is with the Department of Electronic and Electrical Engineering, University of Leeds, Leeds LS2 9JT, U.K.

Publisher Item Identifier S 0018-9456(97)09115-8.

## II. Coaxial Probe Model

The coaxial probe is modeled as a coaxial aperture opening on an infinite ground plane (Fig. 1). This problem is usually addressed by matching the magnetic fields at the aperture. The magnetic field distribution (assuming radial symmetry) in the coaxial region ($z < 0$) with inner conductor radius $a$, outer conductor radius $b$ and relative permittivity of the region between conductors $\varepsilon_c$ is given by [14]

$$H_\phi^-(r,z) = \frac{A_0}{r}[e^{-jk_c z} - \Gamma e^{jk_c z}] + \sum_{n=1}^{\infty} A_n R_n(r) e^{\gamma_n z} \tag{1}$$

where

$$\begin{aligned} k_c &= \omega\sqrt{\varepsilon_c \varepsilon_0 \mu_0} \\ \gamma_n &= \sqrt{\lambda_n^2 - k_c^2} \\ R_n(r) &= \frac{\pi \lambda_n J_0(\lambda_n b)}{\sqrt{2\left(J_0^2(\lambda_n a) - J_0^2(\lambda_n b)\right)}} \\ &\quad \times [J_1(\lambda_n r) Y_0(\lambda_n a) - Y_1(\lambda_n r) J_0(\lambda_n a)] \\ A_0 &= \frac{\varepsilon_c \varepsilon_0 \int_a^b E_r(r,0)\, dr}{k_c \omega (1+\Gamma) \ln\left(\frac{b}{a}\right)} \\ A_n|_{n>0} &= \frac{j\omega\varepsilon_c\varepsilon_0}{\gamma_n} \int_a^b E_r(r,0) R_n(r)\, dr \\ E_r^-(r,z) &= -\frac{j}{\omega\varepsilon_0\varepsilon_c} \frac{\partial H_\phi^-(r,z)}{\partial z}. \end{aligned} \tag{2}$$

The eigenfunctions $R_n(r)$ are expressed in terms of Bessel functions of the first and second kind with order $n$ ($J_n(x)$ and $Y_n(x)$). The eigenvalues ($\lambda_n$) of the eigenfunctions $R_n(r)$ are computed using the transcendental equation

$$J_0(\lambda_n a) Y_0(\lambda_n b) = Y_0(\lambda_n a) J_0(\lambda_n b). \tag{3}$$

In the external region ($z > 0$) with relative permittivity $\varepsilon_m$ the magnetic field is related to the tangential electric field in the aperture ($E_r(r,0)$) [14] of the form

$$H_\phi^+(r,z) = \frac{jk_m^2}{2\pi\omega\mu_0} \int_a^b E_r(r',0) \int_0^{2\pi} \frac{e^{-jk_m R}}{R} r' \cos\psi\, d\psi\, dr' \tag{4}$$

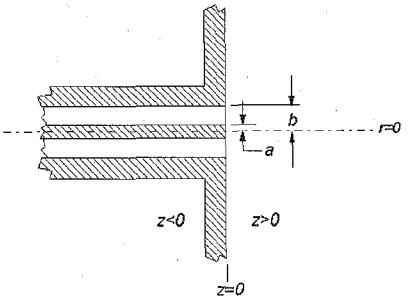


Fig. 1. Geometry of coaxial aperture opening on infinite ground plane.

where

$$k_m = \omega\sqrt{\varepsilon_m \varepsilon_0 \mu_0}$$
$$\psi = (\phi - \phi')$$
$$R = \sqrt{r^2 + r'^2 - 2rr'\cos\psi + z^2}.$$

The solution of the forward problem gives the reflection coefficient ($\Gamma$) for a given permittivity ($\varepsilon_m$). The inverse problem finds the permittivity for a given reflection coefficient. Solutions to both the forward and inverse problems are required for a system to measure permittivity.

A full-wave solution involves variational techniques and is computationally intensive especially when finding the solution to the inverse problem which relies on iterative techniques [6], [15], [16]. When using iterative techniques the speed of the forward solution becomes a limiting factor for practical measurement systems. Often only the principal mode is assumed present when matching the tangential electric fields at the aperture, i.e., $E_r(r,0) = E_0/r$ which leads to faster computation at the expense of accuracy [17]–[19].

A stationary expression is obtained by equating the tangential magnetic field expressions given in (1) and (4) at $z = 0$, multiplying the resulting expression by $rE_r(r,0)$ then integrating from $r = a$ to $r = b$ [14], [18]. Misra uses the simplifying assumption $E_r(r,0) = E_0/r$ to obtain the following expression for the normalized aperture admittance from the stationary expression [19]

$$\tilde{Y}_L = \frac{jk_m^2}{\pi k_c \ln\left(\frac{b}{a}\right)} \int_a^b \int_a^b \int_0^\pi \cos(\phi) \frac{e^{-jk_m R}}{R}\, d\phi\, dr\, dr' \quad (5)$$

where

$$R = \sqrt{r^2 + r'^2 - 2rr'\cos(\phi)}.$$

A Taylor series expansion of the exponential expression in (5) yields an expression where the integrals are independent of the medium characteristics. Once the integrals are computed for a given probe geometry the resulting polynomial expression provides fast computation of the normalized aperture admittance

$$\tilde{Y}_L = \frac{jk_m^2}{\pi k_c \ln\left(\frac{b}{a}\right)} \left\{ j\left[ I_1 - \frac{k_m^2 I_3}{2} + \frac{k_m^4 I_5}{24} - \frac{k_m^6 I_7}{720} + \cdots \right] + \left[ I_2 k - \frac{k_m^3 I_4}{6} + \frac{k_m^5 I_6}{120} - \cdots \right] \right\} \quad (6)$$

where

$$I_n = \int_a^b \int_a^b \int_0^\pi R^{n-2} \cos(\phi)\, d\phi\, dr\, dr' \quad n = 1, 2, 3 \cdots.$$

The admittance computed using (6) deviates from the actual admittance because the higher order modes of the electric field in the aperture are not included in the derivation. A feature of the present work is the empirical modification of the probe constants ($I_n$) with values based on the measurement up to 20 GHz of several known materials with values of permittivity ranging between the permittivity of air and water. Instead of optimizing each parameter individually, the parameters were optimized as a group using the following expression:

$$I_n' = \frac{I_n}{10^{[\alpha+\beta(n-1)+\chi(n-1)^2]}}. \quad (7)$$

Inspection of the relationships between parameters calculated for different geometries revealed a pattern that could be expressed in $\beta$ alone. The $\alpha$ and $\chi$ parameters were added to provide more degrees of freedom for the optimization. The measurements of the known dielectrics were obtained by connecting the probe to the testport of a calibrated vector network analyzer. With a short circuit connected to the probe, the network analyzer calibration was modified using a refresh calibration procedure [20] to establish the measurement reference plane at the probe aperture. The reflection coefficients of the known materials (including air, Teflon, and water) were measured, the optimization parameters ($\alpha, \beta$, and $\chi$) of (7) adjusted until the admittance predicted by (6) provided the best match to each of the measured admittances. Subsequent calculations then used the first 28 modified probe constants ($I_n'$) to model the aperture admittance. The resulting polynomial expression provides a reasonable fit to calculations based on slower variational computations for frequencies less than or equal to $110/\sqrt{\varepsilon_m}$ GHz. Fig. 2 shows an example of the relative accuracy of the polynomial model using both the optimized coefficients ($I_n'$) and the unmodified coefficients ($I_n$). Data for a Cole–Cole model of water at 25 °C with parameters $\varepsilon_s = 78.6$, $\varepsilon_\infty = 4.22$, $\tau = 8.8 \times 10^{-12}$ s and $\alpha = 0.013$ is included for comparison [21]. The Cole-Cole model is

$$\varepsilon = \varepsilon' - j\varepsilon'' = \varepsilon_\infty + \frac{\varepsilon_s - \varepsilon_\infty}{1 + (j\omega\tau)^{1-\alpha}}. \quad (8)$$

The measurements were obtained after a calibration using a fixed load, air, and a short circuit as calibration standards; calibration is described in the next section. The ripples in the measurement are due to the calibration not fully accounting for internal mismatches within the probe (the fixed load is connected in the place of the coaxial probe during the calibration). The imperfections in the fixed load increase with frequency and also slightly degrade the measurement.

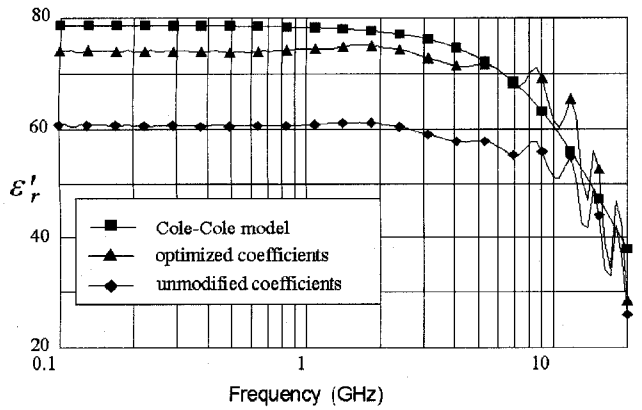


Fig. 2. Comparison of permittivity measurements of water at 25 °C using both optimized probe coefficients ($I'_n$) and unmodified coefficients ($I_n$). Also included is a plot of the Cole–Cole model for water at 25 °C.

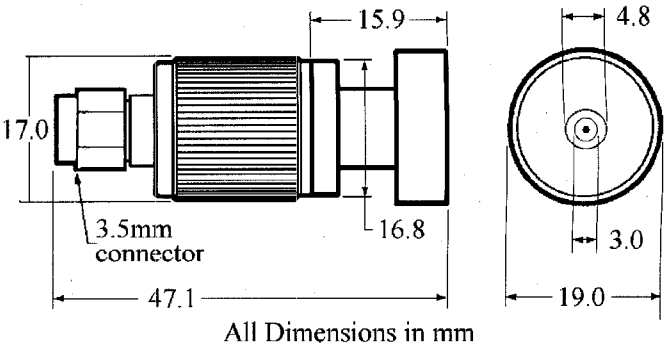


Fig. 3. Coaxial probe with inner diameter of outer conductor = 3.0 mm and diameter of inner conductor = 0.66 mm. The ground plane diameter is 19.0 mm. At a radius of 4.8 mm the ground plane is cut away to a depth of about 0.25 mm to help insure intimate contact between the measurement sample and the coaxial aperture.

## III. Measurement System

A vector network analyzer is used to measure the reflection coefficient from the probe aperture/material interface. The inverse model is then used to compute the permittivity from the reflection coefficient.

The coaxial probe model assumes both an infinite ground plane and semi-infinite sample size. From a practical point of view, these assumptions are justified if reflections from finite boundaries are not sensed at the probe aperture. When measuring lossy samples this criteria is readily satisfied. In other cases a lossy match at the finite boundaries will insure no reflected energy, thereby simulating a semi-infinite sample [8].

The systematic errors of directivity ($e_d$), frequency response ($e_r$), and source match ($e_s$) cause the reflection coefficient measured by the vector network analyzer ($\Gamma_m$) to differ from the actual reflection coefficient ($\Gamma_a$) according to

$$\Gamma_m = e_d + \frac{e_r \Gamma_a}{1 - e_s \Gamma_a}. \tag{9}$$

Calibration (also referred to as vector error correction) corrects for the systematic deviation by measuring three known reflection coefficients enabling a solution for the systematic errors at each measurement frequency. The effects of the systematic errors are then mathematically removed from subsequent measurements [22] yielding the reflection coefficient at the coaxial probe aperture of the form

$$\Gamma_a = \frac{\Gamma_m - e_d}{e_s(\Gamma_m - e_d) + e_r}. \tag{10}$$

All the measurements described in this paper employ this method of error correction.

Others [5], [23], [24] used an alternative to explicitly determining the systematic error terms which relies on the property of invariance of the cross-ratio of complex numbers [25] given by

$$\frac{(\rho_m - \rho_1)(\rho_3 - \rho_2)}{(\rho_m - \rho_2)(\rho_1 - \rho_3)} = \frac{(y_m - y_1)(y_3 - y_2)}{(y_m - y_2)(y_1 - y_3)} \tag{11}$$

where $\rho_1$, $\rho_2$, and $\rho_3$ are the measured coefficients for each of the three calibration standards; $\rho_m$ is the measured reflection coefficient of the unknown sample; $y_1$, $y_2$, and $y_3$ are the admittances of the calibration standards at the probe aperture and $y_m$ is the unknown admittance from which the permittivity is calculated.

Calibration using either (10) or (11) performs a mapping that relies on knowing the reflection coefficients or admittances of some calibration standards. Some have used this mapping to characterize part of the probe model by measuring additional standards [5], [26]. Kraszewski suggested the use of well-known reference liquids as calibration standards for the coaxial probe so that the calibration is easily done at the probe aperture [27]. Using reference liquids as calibration standards imposes the model relating permittivity to aperture admittance on the calibration mapping. The calibration mapping can account for errors in the probe aperture model when measuring materials that are similar to the calibration standards. More accurate models provide better accuracy over a wider range of materials. Nevertheless, using reference liquids as calibration standards has the advantage that the calibration is done at the measurement interface. Air, a short circuit and deionized water are readily available as well-defined calibration materials. The reflection coefficient of a short circuit flush with the probe aperture is $-1$, the reflection coefficients of air and water can be determined using known values of permittivity for each and the forward coaxial probe model. The value of permittivity as a function of frequency for water is accurately known [21], [28].

Deionized water provides a useful standard for the coaxial probe shown in Fig. 3 because the dipole losses of water are sufficient at frequencies where radiation from the probe aperture is appreciable so that the deionized water in a 200 ml beaker more than adequately approximates a semi-infinite sample. There is more difficulty in using deionized water as a calibration standard with larger diameter probes such as the 14 mm diameter probe described in [8] because radiation is prominent at a lower frequency.

After calibration the inverse coaxial probe model is used to determine the permittivity of the sample contacting the coaxial probe from measurements of the coaxial aperture reflection coefficient.

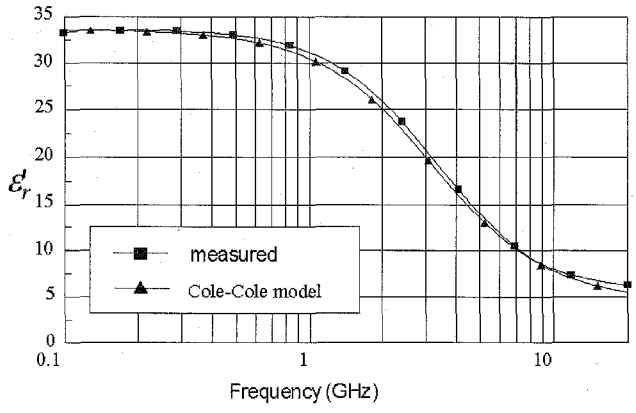


(a)

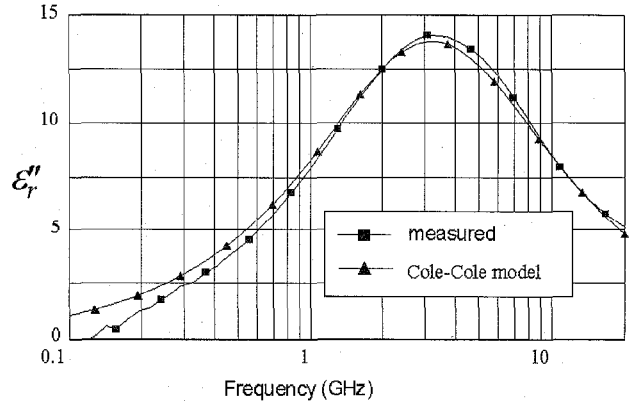


(b)

Fig. 4. Comparison of Debye model with measured values of (a) real part and (b) loss factor of relative permittivity for methanol at 25 °C over a frequency range of 100 MHz to 20 GHz.

Fig. 4(a) and (b) shows measurements of the real part of the relative permittivity ($\varepsilon'$) and the loss factor ($\varepsilon''$) of methanol at 25 °C using the HP85070B coaxial probe (Fig. 3) and the HP8720C vector network analyzer. The measurement system was calibrated using 25 °C deionized water, air, and a short circuit. The measurements compare well to values computed using a Cole–Cole model [see (8)] for methanol [29] with parameters $\varepsilon_s = 33.7$, $\varepsilon_\infty = 4.45$, $\tau = 4.95 \times 10^{-11}$ s, and $\alpha = 0.036$.

Care is taken to avoid changes to the measurement system between calibration and measurement since temperature changes or cable movements introduce perturbations to the systematic errors that will not be accounted for by the calibration. These uncorrected perturbations result in errors in the measured permittivity. An abbreviated calibration procedure known as "refresh cal" can be used to provide a first order correction to the estimates of the systematic errors in a perturbed system from the re-measurement of a single calibration standard [20]. The "refresh cal" procedure benefits from an accurate probe aperture model because it assumes that the calibration mapping accounts for the systematic errors and not a combination of systematic errors and probe aperture model errors.

TABLE I
MEASUREMENT SAMPLES WITH WEIGHT OF DISSOLVED SOLIDS ($w$) DETERMINED BY AN INFRARED TECHNIQUE AND DRY BASIS PERCENTAGE OF FRUCTOSE DETERMINED USING LIQUID CHROMATOGRAPHY

| Samp'ɔ | w (%) | Fruct.(%) | Sample | w (%) | Fruct.(%) |
|---|---|---|---|---|---|
| A | 42.35 | 56.065 | K | 38.00 | 55.551 |
| B | 32.45 | 54.711 | L | 46.70 | 55.465 |
| C | 37.60 | 55.254 | M | 35.15 | 55.482 |
| D | 33.40 | 56.608 | N | 33.30 | 55.195 |
| E | 41.20 | 55.877 | O | 34.70 | 55.950 |
| F | 44.95 | 55.687 | P | 38.20 | 55.685 |
| G | 33.60 | 55.398 | Q | 38.35 | 55.293 |
| H | 43.40 | 55.861 | R | 38.35 | 55.745 |
| I | 41.25 | 55.620 | S | 37.15 | 55.622 |
| J | 42.00 | 55.537 | T | 38.50 | 55.880 |

## IV. MEASUREMENT OF TEST SOLUTIONS

Twenty corn syrup samples were measured. The measurement samples consisted of varying amounts of dissolved solids in water. Table I indicates the percent by weight of dissolved solids ($w$) in each sample ranging from 32.45% in sample B to 46.7% in sample L. The dry basis percentage of fructose is also indicated (Fruct). The other dissolved solids consisted of dextrose and maltose. The percentage of dissolved solids were independently determined by an infrared refractive index technique with a standard deviation of 0.15–0.2%. The fructose measurement was made using a liquid chromatography with a standard deviation of 0.15%.

Temperature variations in polar materials are known to change the permittivity; prior to measurement the samples were stabilized in a water bath to ensure that all samples were at the same 25 °C temperature. The network analyzer was turned on and allowed to stabilize for 1 h prior to use to reduce any effects from internal thermal drift. The coaxial probe was rigidly mounted on a fixture to minimize measurement errors that can be introduced through cable movement between calibration and measurement.

A calibration of the coaxial probe/network analyzer system using air, short circuit and 25 °C water was performed and then each of the twenty samples was measured four times. The permittivity of air was measured at the start of the measurement sequence and again at the end of the sequence to verify that a minimal system drift occurred between calibration and the measurement of each sample. The entire process was repeated on another day using the same calibration and measurement techniques.

### A. Curve Fitting Technique

The measured data was fitted to (12) which includes three relaxation times ($\tau_1, \tau_2, \tau_3$). It was assumed that multiple relaxations would occur in the solutions and three parameters were found to provide a better empirical fit to the measured data than two. The coefficients of the following expression were optimized for best fit to the measured data using a modified version of the Levenberg–Marquardt method [30]

$$\varepsilon(\omega) = \varepsilon_4 + \frac{\varepsilon_1 - \varepsilon_2}{1 + j\omega\tau_1} + \frac{\varepsilon_2 - \varepsilon_3}{1 + j\omega\tau_2} + \frac{\varepsilon_3 - \varepsilon_4}{1 + j\omega\tau_3}. \quad (12)$$

There is not adequate sensitivity to discriminate $\varepsilon_4$ since only part of the highest frequency polar response is included in the measurement frequency range. The expected value of $\varepsilon_4$ would be in the range 1 to 5; any value in that range will provide an adequate fit. Results below have the value of $\varepsilon_4$ fixed to 1. The remaining model parameters $(\varepsilon_1, \varepsilon_2, \varepsilon_3, \tau_1, \tau_2, \tau_3)$ in (12) are normalized to avoid ill-conditioned matrices. New model coefficients were defined $(\mathbf{a} = [a_1, a_2, a_3, a_4, a_5, a_6])$ and initialized to unity. The new coefficients were allowed to vary during the optimization while the model parameters became normalization constants. Adding the normalizing coefficients to (12) yields

$$\varepsilon(\omega;\mathbf{a}) = \varepsilon'(\omega;\mathbf{a}) - j\varepsilon''(\omega;\mathbf{a}) = 1 + \frac{a_1\varepsilon_1 - a_2\varepsilon_2}{1 + j\omega a_4\tau_1} + \frac{a_2\varepsilon_2 - a_3\varepsilon_3}{1 + j\omega a_5\tau_2} + \frac{a_3\varepsilon_3 - 1}{1 + j\omega a_6\tau_3}. \quad (13)$$

Since the measured and modeled data was complex the merit function had to be modified as follows to include both the real and imaginary parts

$$\chi^2(\mathbf{a}) = \sum_{i=1}^{N} \left[ \frac{(\varepsilon_i' - \varepsilon'(\omega_i;\mathbf{a}))^2 + (\varepsilon_i'' - \varepsilon''(\omega_i;\mathbf{a}))^2}{\sigma_i^2} \right]. \quad (14)$$

The inverse solution of the coaxial probe model is an iterative technique that computes permittivity from a measured reflection coefficient. The inverse solution also provides sensitivity numbers $(S_i)$ which are defined as

$$S_i = \left| \frac{\Delta\varepsilon_r}{\Delta\Gamma_a} \right|.$$

Errors due to noise or drift in the measurement of the reflection coefficient map into permittivity measurement errors $(\sigma_i)$ proportional to the sensitivity of the coaxial probe so an appropriate relative weighting of the measurement data is provided by setting $\sigma_i = S_i$.

### B. Measurement Results

Each of the 20 samples were measured eight times then curve fitted using the Levenberg–Marquardt method outlined above. Fig. 5 shows the measured and curve fitted results of both the real part of the relative permittivity $(\varepsilon')$ and the loss factor $(\varepsilon'')$ for sample A; the remaining samples provided an equally good fit. The resulting coefficients were then fitted to either a linear regression $(\varepsilon_i = a + w \cdot b)$ or to an exponential regression $(\tau = ae^{w \cdot b})$ where $w$ is the weight of the dissolved solids expressed in percentage of the sample's total mass. Table II provides the regression coefficients for each of the parameters. With the exception of $\tau_1$ the fits are nearly perfect. There is a small offset bias between the two sets of measurements made on different days; the regression coefficient of $\tau_1$ is principally effected. Each of the two sets of measurements, taken independently, yields a regression coefficient for $\tau_1$ better than 0.94. One or more of the individual model parameters could be used as a gauge for the percentage of dissolved solids. However, a better measure is obtained by taking a linear combination of all the model parameters.

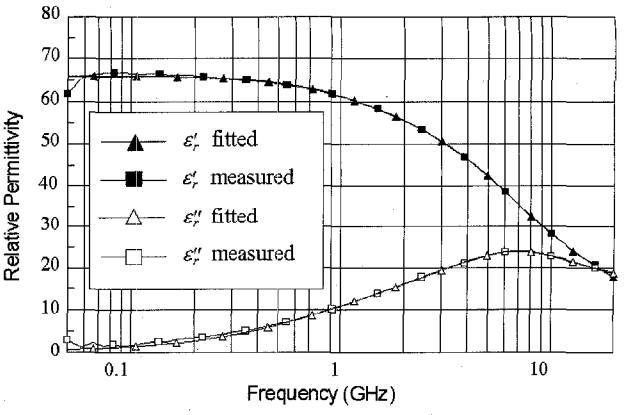


Fig. 5. Measured and fitted expression of complex relative permittivity for fructose sample A.

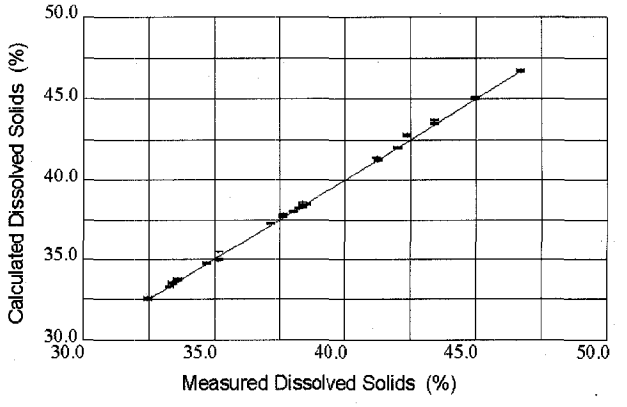


Fig. 6. Comparison of percent dissolved solids measured by fructose manufacturer and percent dissolved solids computed from linear combination of parameters of permittivity expression given in (12). Samples K, L, N, and O were used to computed the linear coefficients $[c_1 \cdots c_6]$ used in (15).

TABLE II
REGRESSION COEFFICIENTS FOR THE MODEL PARAMETER VARIATION [SEE (12)] AS A FUNCTION OF DISSOLVED SOLIDS. EACH PARAMETER IS FITTED USING EITHER A LINEAR REGRESSION $(\varepsilon_i = a + w \cdot b)$ OR AN EXPONENTIAL REGRESSION $(\tau = ae^{w \cdot b})$ WHERE $w$ IS THE WEIGHT OF THE DISSOLVED SOLIDS EXPRESSED IN PERCENTAGE OF THE SAMPLE'S TOTAL MASS

| $y$ | $a$ | $b$ | $r^2$ | type |
|---|---|---|---|---|
| $\varepsilon_1$ | 82.3 | -0.3847 | 0.99391 | linear |
| $\varepsilon_2$ | 91.4 | -0.8506 | 0.99623 | linear |
| $\varepsilon_3$ | 39.2 | -0.5354 | 0.98181 | linear |
| $\tau_1$ | 6.70E-11 | 0.01294 | 0.65714 | exponential |
| $\tau_2$ | 1.10E-11 | 0.01702 | 0.98478 | exponential |
| $\tau_3$ | 8.00E-12 | -0.0180 | 0.92352 | exponential |

The following expression was used to compute the percentage of dissolved solids from the fitted parameters

$$w = c_1 + c_2\varepsilon_1 + c_3\varepsilon_2 + c_4\varepsilon_3 + c_5\ln(\tau_1) + c_6\ln(\tau_2) + c_7\ln(\tau_3). \quad (15)$$

Four samples (samples K, L, N, and O) were chosen to compute the coefficients ($c_i$). The permittivity parameters from the measurements of the four samples (total of 32 measurements) and the value of percentage of dissolved solids measured by the supplier for those samples were used in the following equation to obtain a least squares fit for the coefficients in (15):

$$\begin{bmatrix} c_1 \\ c_2 \\ c_3 \\ c_4 \\ c_5 \\ c_6 \\ c_7 \end{bmatrix} = \begin{bmatrix} 1 & \varepsilon_{11} & \varepsilon_{21} & \varepsilon_{31} & \ln(\tau_{11}) & \ln(\tau_{21}) & \ln(\tau_{31}) \\ \vdots & \vdots & \vdots & \vdots & \vdots & \vdots & \vdots \\ 1 & \varepsilon_{1n} & \varepsilon_{2n} & \varepsilon_{3n} & \ln(\tau_{1n}) & \ln(\tau_{2n}) & \ln(\tau_{3n}) \end{bmatrix}^{-1} \times \begin{bmatrix} w_1 \\ \vdots \\ w_n \end{bmatrix}. \quad (16)$$

Once the coefficients were computed, the percentage of dissolved solids was computed for each measurement using (15). Fig. 6 compares the computed percentage of dissolved solids with the values independently measured by the supplier of the samples using an independent, nonmicrowave, technique. The two techniques track each other very accurately to within the repeatability of the measurements. The average difference between the values provided by the supplier and the computed values is 0.08% with a standard deviation of 0.13%. The standard deviation of the calculated dissolved solids derived from permittivity measurements is consistent with the standard deviation of the infrared technique used by the manufacturer to characterize the samples.

During the measurements of the solutions care must be taken to maintain a constant sample temperature. Temperature variation will affect the measured permittivity. Since the fitted expression uses multiple parameters the possibility exists of determining more than one material property such as dissolved solids percentage and temperature.

## V. Conclusion

Enhancements to a model for the coaxial probe provides the basis for extending the useful range of permittivity measurements without sacrificing computational speed or accuracy. Computations of permittivity at 201 different frequencies from reflection coefficient measurements take less than 4 s on a 33 MHz 486 DX PC. Permittivity measurements made with the coaxial probe can provide a concise representation of the functional dependence of permittivity on frequency. The parameters from such a concise representation provide a useful gauge for some material properties such as moisture content. Using the technique to evaluate the percentage of dissolved solids in a solution, the accuracy of the measurement is similar to the accuracy obtained with infrared techniques.

## Acknowledgment

The authors gratefully acknowledge Cargill Inc. for providing both the measurement samples and the independent infrared characterization of the percentage of dissolved solids.

## References

[1] E. C. Burdette, F. L. Cain, and J. Seals, "In vivo probe measurement technique for determining dielectric properties at VHF through microwave frequencies," *IEEE Trans. Microwave Theory Tech.*, vol. MTT-28, pp. 414–427, Apr. 1980.

[2] T. W. Athey, M. A. Stuchly, and S. S. Stuchly, "Measurement of radio frequency permittivity of biological tissues with an open-ended coaxial line: Part I," *IEEE Trans. Microwave Theory Tech.*, vol. MTT-30, pp. 82–86, Jan. 1982.

[3] G. Gajda and S. S. Stuchly, "An equivalent circuit of an open-ended coaxial line," *IEEE Trans. Instrum. Meas.*, vol. IM-32, pp. 506–509, Dec. 1981.

[4] M. A. Stuchly, M. M. Brady, S. S. Stuchly, and G. Gajda, "Equivalent circuit of an open-ended coaxial line in a lossy dielectric," *IEEE Trans. Instrum. Meas.*, vol. IM-31, pp. 116–119, June 1982.

[5] T. P. Marsland and S. Evans, "Dielectric measurements with an open-ended coaxial probe," *Proc. IEE*, vol. 134, pt. H, pp. 341–349, Aug. 1987.

[6] R. D. Nevels, C. M. Butler, and W. Yablon, "The annular slot antenna in a lossy biological medium," *IEEE Trans. Microwave Theory Tech.*, vol. MTT-33, pp. 314–319, Apr. 1985.

[7] C.-L. Li and K.-M. Chen, "Determination of electromagnetic properties of materials using flanged open-ended coaxial probe—Full wave analysis," *IEEE Trans. Instrum. Meas.*, vol. 44, pp. 19–27, Feb. 1995.

[8] J. P. Grant, R. N. Clarke, G. T. Symm, and N. M. Spyrou, "A critical study of the open-ended coaxial line sensor technique for RF and microwave complex permittivity measurements," *J. Phys. E: Sci. Instrum.*, vol. 22, pp. 757–770, 1989.

[9] P. De Langhe, L. Martens, and D. De Zutter, "Design rules for an experimental setup using an open-ended coaxial probe based on theoretical modeling," *IEEE Trans. Instrum. Meas.*, vol. 43, pp. 810–817, Dec. 1994.

[10] D. Misra, "On the measurement of the complex permittivity of materials by an open-ended coaxial probe," *IEEE Microwave Guided Wave Lett.*, vol. 5, pp. 161–163, 1995.

[11] S. S. Stuchly, C. L. Sibbald, and J. M. Anderson, "A new aperture admittance model for open-ended waveguides," *IEEE Trans. Microwave Theory Tech.*, vol. 42, pp. 192–198, Feb. 1994.

[12] J. M. Anderson, C. L. Sibbald, and S. S. Stuchly, "Dielectric measurements using a rational function model," *IEEE Trans. Microwave Theory Tech.*, vol. 42, pp. 199–204, Feb. 1994.

[13] A. Kraszewski, "Microwave aquametry—A review," *J. Microw. Power*, vol. 15, pp. 209–220, 1980.

[14] H. Levine and C. H. Papas, "Theory of the circular diffraction antenna," *J. Appl. Phys.*, vol. 22, pp. 29–43, 1951.

[15] J. R. Mosig, J.-C. E. Besson, M. Gex.-Fabry, and F. E. Gardiol, "Reflection of an open-ended coaxial line and application to nondestructive measruements of materials," *IEEE Trans. Instrum. Meas.*, vol. IM-30, pp. 46–51, Mar. 1981.

[16] T. E. Hodgetts, "The open-ended coaxial line: A rigorous variational treatment," memo. 4331, Royal Signals Radar Establishment, Great Malvern, Worcestershire, U.K., 1989.

[17] N. Marcuvitz, "Lines radiating into space," in *Waveguide Handbook*, N. Marcuvitz, Ed. New York: McGraw-Hill, 1951, pp. 213–216.

[18] J. Galejs, "Slot antennas in free space," in *Antennas in Inhomogenous Media*, J. Galejs, Ed. New York: Pergamon, 1969, pp. 33–45.

[19] D. Misra, "A quasistatic analysis of open-ended coaxial lines," *IEEE Trans. Micrwave Theory Tech.*, vol. MTT-35, pp. 925–928, Oct. 1987.

[20] D. V. Blackham, "Calibration method for open-ended coaxial probe/vector network analyzer system," in *Microwave Processing of Materials III*, R. L. Beatty, W. H. Sutton, and M. F. Iskander, Eds.. Pittsburgh, PA: Materials Res. Soc., 1992, vol. 269, pp. 595–599.

[21] J. B. Hasted, "Liquid water: Dielectric properties," in *The Physics and Physical Chemistry of Water: Water—A Comprehensive Treatise*, F. Franks, Ed. New York: Plenum, 1972, vol. 1, ch. 7, pp. 255–309.

[22] J. Fitzpatrick, "Error models for systems measurement," *Microwave J.*, vol. 21, pp. 63–66, May 1978.

[23] D. Misra, M. Chabbra, B. R. Epstein, M. Mirotznik, and K. R. Foster, "Nonivasive electrical characterization of materials at microwave frequencies using an open-ended coaxial line: Test of an improved calibration technique," *IEEE Trans. Microwave Theory Tech.*, vol. 38, pp. 8–14, Jan. 1990.
[24] Y.-Z. Wei and S. Sridhar, "Radiation-corrected open-ended coax line technique for dielectric measurements of liquids up to 20 GHz," *IEEE Trans. Microwave Theory Tech.*, vol. 39, pp. 526–531, Mar. 1991.
[25] R. W. Beatty, *Invariance of the Cross Ratio Applied to Microwave Network Analysis*, NBS Tech. Note 623, National Bureau of Standards, U.S. Department of Commerce, Boulder, CO, 1972.
[26] K. F. Staebell and D. K. Misra, "An experimental technique for in vivo permittivity measurement of materials at microwave frequencies," *IEEE Trans. Microwave Theory Tech.*, vol. 38, pp. 337–339, Mar. 1990.
[27] A. Kraszewski, M. A. Stuchly, and S. S. Stuchly, "ANA calibration method for measurements of dielectric properties," *IEEE Trans. Instrum. Meas.*, vol. IM-32, pp. 385–386, June 1983.
[28] P. O. Risman, "Microwave properties of water in the temperature range +3 to +140 °C," *Electromag. Energy Rev.*, vol. 1, no. 2, pp. 8–10, 1988.
[29] B. P. Jordan, R. J. Sheppard, and S. Szwarnowski, "The dielectric properties of formamide, ethanediol and methanol," *J. Phys. D: Appl. Phys.*, vol. 11, pp. 695–701, 1978.
[30] W. H. Press, B. P. Flannery, S. A. Teukolsky, and W. T. Vetterling, "Modeling of data," in *Numerical Recipes in C*, B. P. Flannery, S. A. Teukolsky, and W. T. Vetterling, Eds. Cambridge, U.K.: Cambridge Univ. Press, 1988, pp. 517–565.

**David V. Blackham** (S'79–M'85) was born in Salt Lake City, UT, in 1954. He received the B.S.E.E. degree from Brigham Young University, Provo, UT, the M.S.E.M. degree from Stanford University, Stanford, CA, the M.S.E.E. degree from National Technological University, Fort Collins, CO, and is currently pursuing the Ph.D. degree from the University of Leeds, Leeds, U.K.

He has been an R&D Engineer with Hewlett-Packard since 1979, where he has worked on the HP8340A Synthesized Sweeper, scalar detectors and bridges, RF and microwave vector network analyzers, and microwave characterization of materials. His current interests include vector error correction and measurement accuracy associated with vector network analyzers.

**Roger D. Pollard** (M'77-SM'91-F'97) was born in London, U.K., in 1946. He received the B.Sc. and Ph.D. degrees in electrical and electronic engineering from the University of Leeds, Leeds, U.K.

He holds the Hewlett-Packard Chair in High Frequency Measurements in the Department of Electronic and Electrical Engineering at the University of Leeds where he has been a faculty member since 1974. He is jointly responsible for the activities of the Microwave and Terahertz Technology Research Group which has over 40 active researchers, a strong graduate program and has made contributions to microwave passive and active device research. The activity has significant industrial collaboration as well as a presence in continuing education through its Microwave Summer School. His personal research interests are in microwave network measurements, calibration and error correction, microwave and millimiter-wave circuits, and large-signal and nonlinear characterization. He has been a consultant to the Hewlett-Packard Company, Santa Rosa, CA, since 1981.

Dr. Pollard is a Chartered Engineer and a member of the Institution of Electrical Engineers (U.K.). He is serving his second term as an elected member of the IEEE MTT-S Administrative Committee, where he is 1997 Vice President.